physica status solidi pss rrl
www.pss-rapid.com

Systematic Investigation on the Surfactant-Assisted Liquid-Phase Exfoliation of MoS_2 and WS_2 in Water for Sustainable 2D Material Inks

Micaela Pozzati, Felix Boll, Matteo Crisci, Sara Domenici, Bernd Smarsly, Teresa Gatti, and Mengjiao Wang**

MoS_2 and WS_2 have gathered significant attention due to their tunable properties and wide range of applications. Liquid-phase exfoliation (LPE) is a facile method to prepare 2D MoS_2 and WS_2. Currently, the principally employed solvents for LPE of MoS_2 and WS_2 are expensive and toxic, and have high boiling points. These drawbacks encourage to find more sustainable alternatives to the liquid medium used for the preparation of 2D material inks. Water is the best option, but surfactants are necessary for LPE in water, since MoS_2 and WS_2 are hydrophobic. Organic molecules with amphoteric character such as sodium dodecyl sulfate, sodium dodecylbenzene sulfonate, and sodium hexadecyl sulfonate (SHS) are selected as suitable candidates for the role. However, the study of these surfactants used in LPE is barely systematically reported. In this work, a detailed investigation is presented on their impact on the LPE of MoS_2 and WS_2, which are representatives of transition-metal dichalcogenides. By characterizing and qualifying the products from average number of layers, it is found that all the surfactants work efficiently to exfoliate MoS_2 and WS_2 into few layers, and SHS stabilizes the 2D layers better than the other two. However, in terms of yield and relative surfactant concentration, a real trade-off is not identified between maximized quantity of exfoliated materials and minimized surfactant concentration, which prompts to select the colloidal ink based on the specific further needs for processing.

1. Introduction

Transition-metal dichalcogenides (TMDs) have gathered significant attention in a wide range of applications, such as energy storage, sensing, and optoelectronics.[1–3] In this broad family of materials, MoS_2 and WS_2 play important roles due to the possibility of preparing the 2D layered counterparts, which possess specific electronic and optical properties.[4–7] As shown in **Figure 1**, MoS_2 and WS_2 contain a layer of metal atoms sandwiched between two sulfur layers, and these sandwiched layers are linked to each other by van der Waals (vdW) forces in the bulk.[8–12] Due to the unique layered structure, it is possible to use top-down methodologies which are more scalable, versatile, and cost-effective compared to the bottom-up methods.[9] Therein, liquid-phase exfoliation (LPE) is commonly used to produce 2D layered materials. This procedure consists in delaminating the layers of the material dispersed in a solvent by mechanical forces such as ultrasonication and high shear mixing.[13] For instance, in the sonication-assisted LPE, the sonication generates the growth and collapse of microbubbles of the solvents, thus resulting in shock waves. These waves can produce shear forces on the bulk materials, break the vdW interactions between the layers of the 2D structures, and form layered materials eventually.[14,15] The type of solvent plays an important role on the yield and quality of the 2D materials. Typically, organic solvents such as N-methyl-2-pyrrolidone, dimethyl sulfoxide, and *N,N*-dimethyl formamide are the most commonly used in exfoliating MoS_2 and WS_2. However, they are expensive and toxic, and have high boiling point.[16–18] To avoid these disadvantages, water is applied as an alternative. Since most of the TMDs are hydrophobic, surfactants are needed to stabilize the 2D nanocrystals in water.

In LPE, ionic surfactants are applied for stabilizing the samples and thus increase the production yield in 2D layered colloids in water.[19,20] Thanks to the electrostatic forces, the ionic surfactants can compensate the vdW attraction between the layers of the material, thus preventing the restacking.[21,22] There are different kinds of surfactants that can be used in this process and

M. Pozzati, S. Domenici, T. Gatti, M. Wang
Dipartimento Scienza Applicata e Tecnologia (DISAT)
Politecnico di Torino
Corso Duca degli Abruzzi 24, 10129 Torino, Italy
E-mail: teresa.gatti@polito.it; mengjiao.wang@polito.it

F. Boll, M. Crisci, B. Smarsly, T. Gatti
Center for Materials Research (LaMa)
Justus Liebig University
Heinrich-Buff-Ring 17, 35392 Giessen, Germany

The ORCID identification number(s) for the author(s) of this article can be found under https://doi.org/10.1002/pssr.202400039.

DOI: 10.1002/pssr.202400039

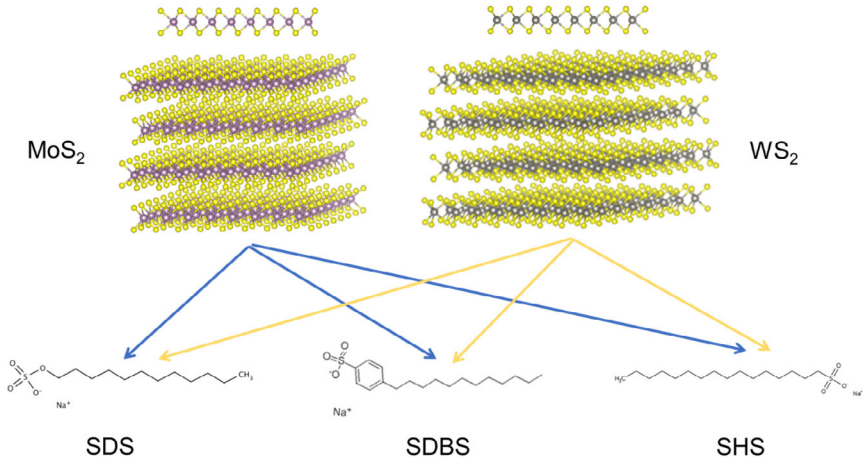

Figure 1. Structures of the two-layered TMDs considered in this study (MoS_2 and WS_2) in their semiconducting H-phase and modular structures of surfactants SDS, SDBS, and SHS.

the most reported one for MoS_2 and WS_2 is an anionic surfactant, namely sodium dodecyl sulfate (SDS), whose chemical structure is shown in Figure 1b.[23] It is characterized by a C_{12} alkyl chain that tends to aggregate on the nanosheets surface, avoiding the restacking.[20,24] Surfactants with a similar structure as SDS have been applied in LPE as well. Sodium dodecylbenzene sulfonate (SDBS) is also used as stabilizing agent. It is reported that the nonpolar benzene rings in SDBS combine with the 2D layers with a strong bind energy, thus improving at the same time the colloidal stability and yield in 2D MoS_2 in an aqueous solution.[25,26] Additionally, since it is reported that the length of the alkyl chain can have an impact on the stability of the dispersion, we have identified sodium hexadecyl sulfonate (SHS) as a new potential surfactant for stabilizing 2D nano-inks, considering its long C_{16} alkyl chain.[27] Plenty of previous studies suggest that the concentration of the surfactant has a great impact on the dispersion quality and final concentration.[20] Therefore, to tune, the concentration of the surfactants will be important for optimizing the LPE of MoS_2 and WS_2.

In this work, we perform a systematic investigation about the influence of the surfactant type and concentration on the quality of exfoliated MoS_2 and WS_2. As shown in Figure 1, three different surfactants, SDS, SDBS, and SHS have been selected for this study. These organic surfactants have a critical micellar concentration (CMC), and it was reported that surfactants can play a more efficient role in LPE when their concentration is less than the CMC.[28] However, some other reports have shown that the surfactant concentration has negligible influence on the yield and quality of exfoliated samples.[23] This confliction encourages us to systematically investigate the relationship between surfactant concentration and the exfoliated samples by LPE. Considering the CMC of SDS, SDBS, and SHS are respectively 8.2, 2.7, and 0.55 mM,[29–32] we chose the CMC of SDS as the highest surfactant concentration and set the concentrations to 8.2, 4.1, 2.0, 1.0, and 0.5 mM for comparison. By testing the UV–vis absorption, Raman spectra, zeta potential (ZP), we were able to compare the quality of the exfoliated MoS_2 and WS_2 in the aspect of layer thickness and stability. Eventually, the production yield is calculated for all the exfoliated samples. It is found that the thickness of the layers is not tightly related to the surfactant type and concentration, as almost all the samples are few layered for MoS_2 and mostly monolayered for WS_2. Meanwhile, SHS performs better than the other two surfactants in stabilizing the nanosheets, since LPE MoS_2 and WS_2 colloids have long-term stability with SHS.

2. Results and Discussion

The suspensions of MoS_2 and WS_2 were obtained with the surfactant-assisted LPE method described in Experimental Section, and the MoS_2 or WS_2 samples were labeled by the surfactant type and concentration. Transmission electron microscope (TEM) measurements were performed on selected MoS_2 and WS_2 suspensions to characterize the morphology of the exfoliated samples in detail. In **Figure 2**a, it is evident that the exfoliated MoS_2 are thin nanosheets with a lateral size of more than 500 nm. In Figure 2b, the TEM image with higher magnification displays a thin side view of less than 10 nm of the nanosheets. Since the interlayer spacing of MoS_2 is 0.615 nm, we expect that the exfoliated samples have less than 16 layers.[33] Figure 2c shows a TEM image of the exfoliated WS_2 nanosheets of more than 500 nm lateral size. In Figure 2d, it is easy to find the thickness of the WS_2 nanosheets of around 5 nm from the wrinkled part, which implies that the obtained WS_2 nanosheets have less than 8 layers.[34]

The effect of the surfactant on the optical properties of exfoliated MoS_2 was studied by UV–vis absorption spectroscopy. **Figure 3** shows the UV–vis normalized absorption spectra of LPE MoS_2 with SDS, SDBS, and SHS at different concentrations. All the spectra have shown the four characteristic excitons of MoS_2 at around 670 nm for the A exciton, 610 nm for the B exciton, 450 nm for the C exciton, and 395 nm for the D exciton, confirming the existence of the 2D layered material. Spectral changes are observed while varying the concentration of the surfactant. Therein, *A* and *B* excitons stands for direct excitonic transitions occurring at the *K* points in the first Brillouin zone, due to

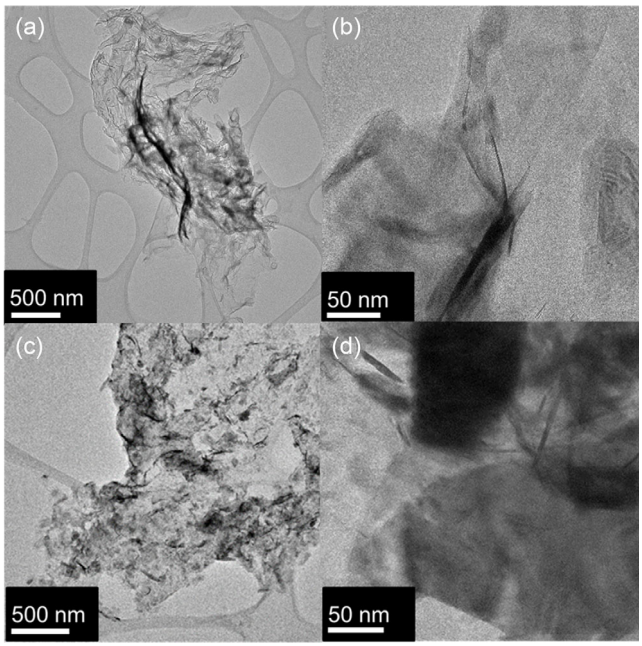

Figure 2. TEM images of a,b) MoS_2 SDBS 1.0 mM and c,d) WS_2 SDS 0.5 mM.

the spin–orbit splitting of the top of the valence band. *C* and *D* excitons are related to the optical transitions from the deep valence band to the conduction band.[35] In Figure 3a, the slope in the region between the *B* exciton and the *C* exciton becomes sharper while increasing the surfactant concentration, indicating smaller and thinner nanosheets. In addition, the value of *A* exciton is closely related to the size of the product. As listed in **Table 1**, the position of the *A* exciton tends to shift to shorter wavelength while increasing the concentration, revealing smaller and thinner nanosheets as well.[20,36–38] It has to be mentioned that there is no linear relationship between ligand concentration and absorption intensity, since the linear increase of surfactant concentration does not result in the linear increase of sample concentration, which have direct influence on the absorbance intensity. While the relationship between product yield and concentration of the surfactant will be discussed in the following content.

In addition, the bandgap of the nano-colloids was calculated with the Tauc plot equation (Equation (1)):

$$(\alpha h\nu)^{1/n} = A\,(h\nu - E_g) \tag{1}$$

where α is the absorption coefficient, h is the Plank constant, ν is the frequency, E_g is the bandgap energy, and n is 2 for the indirect bandgap materials such as few-layered MoS_2 and WS_2.[39] The values obtained are listed in Table 1. It is obvious that all the exfoliated MoS_2 have a larger bandgap range of 1.38–1.65 eV compared to the bulk MoS_2 (1.2 eV).[40] When comparing values between different surfactants, SHS in general results in higher bandgap compared to other surfactants, which means MoS_2 can be exfoliated into thinner layers when SHS is applied. While comparing the values between different concentration of the same surfactant, higher concentration of surfactant tends to produce the samples with higher bandgap, which means thinner nanosheets.[41] At last, the MoS_2 SHS 8.2 mM sample features the broadest bandgap of 1.65 eV, which means it likely contains nanosheets with the smallest average number of layers among all the LPE MoS_2 samples.

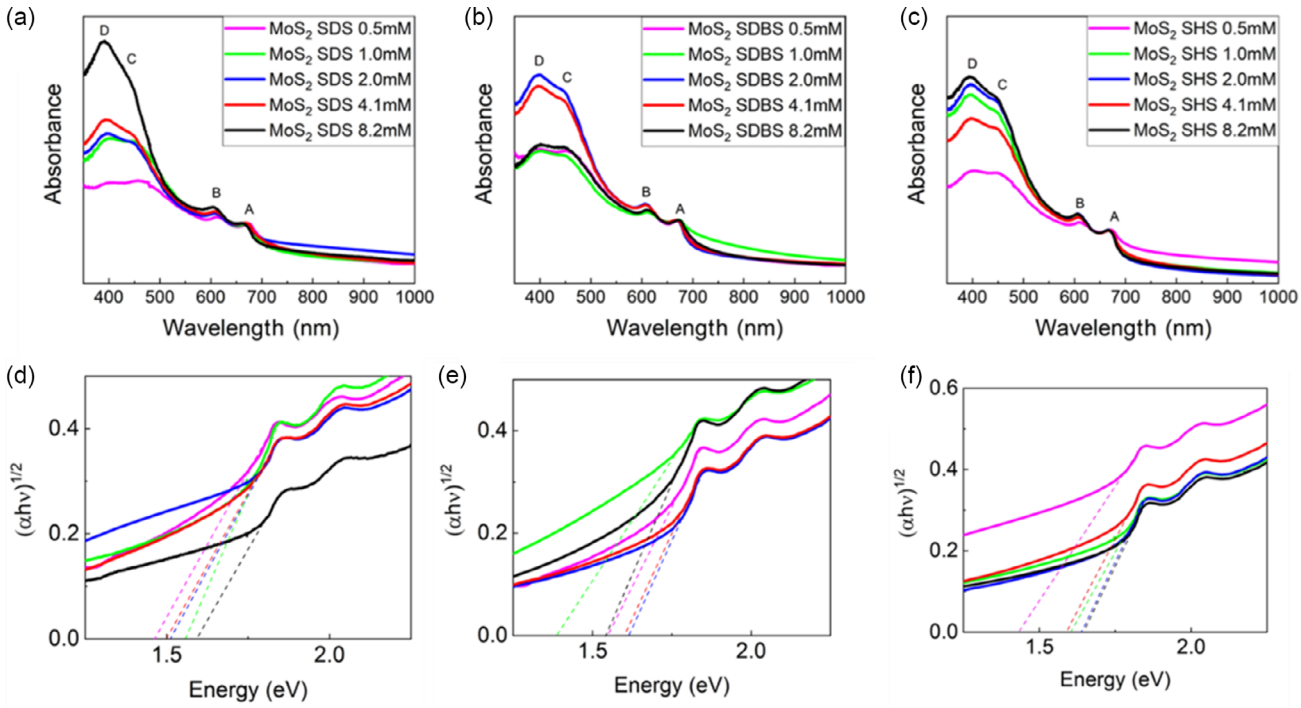

Figure 3. UV–Vis absorption spectra and corresponding Tauc plots of exfoliated MoS_2 with a,d) SDS, b,e) SDBS, and c,f) SHS.

Table 1. Positions of A exciton and bandgap values for LPE MoS_2 samples with the three different surfactants.

Surfactant	Surfactant concentration [mM]	A exciton [nm]	Bandgap [eV]
	8.2	664.6	1.59
	4.1	671.1	1.50
SDS	2.0	668.9	1.51
	1.0	671.1	1.56
	0.5	673.4	1.46
	8.2	672.1	1.54
	4.1	670.1	1.60
SDBS	2.0	667.8	1.62
	1.0	672.1	1.38
	0.5	672.2	1.55
	8.2	667.8	1.65
	4.1	668.9	1.58
SHS	2.0	668.9	1.64
	1.0	669.3	1.61
	0.5	672.2	1.43

The UV–vis spectra of WS_2 are shown in **Figure 4**a–c. We can observe the presence of the four characteristic excitons of WS_2 (*A*: ≈630 nm; *B*: ≈522 nm; *C*: ≈460 nm; and *D*: ≈430 nm) in all the spectra while varying the surfactant type and concentration, revealing the success of exfoliation in all the experiments.[38] Specifically, in Figure 4d, it is shown that the bandgap of exfoliated WS_2 increases from 1.42 to 1.74 eV with the increasing concentration of SDS from 0.5 to 8.2 mM. Therefore, higher concentration of SDS results in the exfoliated WS_2 with broad bandgap and thinner layers of the samples on average. In contrast, for SDBS and SHS, difference in concentration has negligible influence on the bandgap of the samples, as shown in Figure 4e,f, and the bandgap of the samples by SDBS and SHS is around 1.74 eV. However, there is an exception of WS_2 SHS 8.2 mM, which shows a bandgap of 1.43 eV. This might be because 8 mM is much more than the suitable concentration of SHS to exfoliate WS_2 and results in thicker layers than other concentrations. Although the concentrations from 0.5 to 4.1 mM are all more than the CMC of SHS (0.5 mM), we still obtained WS_2 thin layers. It means that for the exfoliation of WS_2 with SHS, the concentration of SHS is not limited to the CMC. This result is different from the exfoliation of MoS_2 with SHS, which all results in thick MoS_2 layers, as shown in Table 1. This might be because the different hydrophobicity of WS_2 and MoS_2 results in different interaction intensity between the TMDs and SHS.[42] All the A-exciton positions and bandgap values are listed in **Table 2**, for the sake of comparison.

Exfoliation from the bulk to a 2D layered material results in a change of chemical structure and electronic properties on the surface of the samples. Therefore, Raman spectroscopy is used as an effective technique for identifying the change in surface chemical bonding and characterizing these exfoliated MoS_2 and WS_2. As shown in **Figure 5**a–c, all the exfoliated MoS_2 samples display two characteristic peaks: the peak at around 383 cm^{-1} is assigned to the E_{2g} mode, while the peak at around 408 cm^{-1} is assigned to the A_{1g} mode.[43,44] E_{2g} and A_{1g} are related to the in-plane and out-of-plane vibrations within the stacked layers. The shift between the two peak positions at ≈383 and ≈408 cm^{-1} can be used to identify the number of layers in that exfoliated MoS_2 particles, since the thickness of the materials is correlated with the frequency.[43–46]

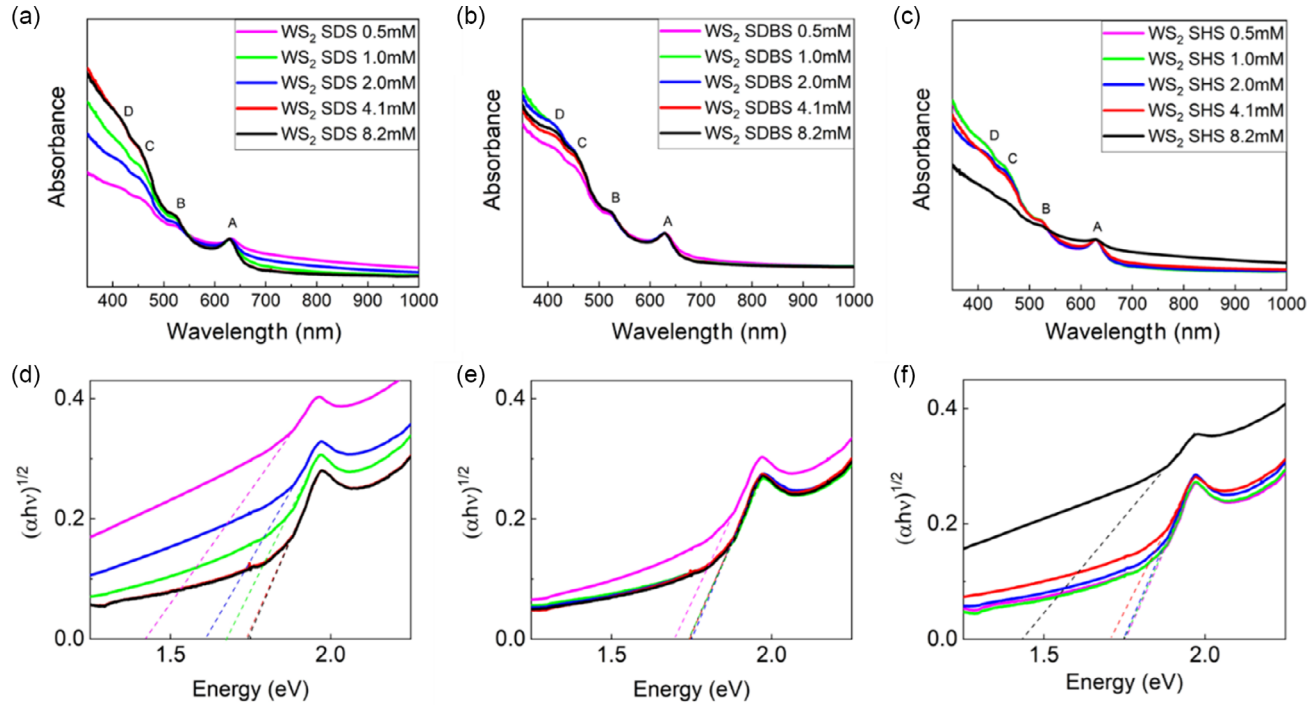

Figure 4. UV–Vis absorption spectra and corresponding Tauc plots of exfoliated WS_2 with a,d) SDS, b,e) SDBS, and c,f) SHS.

Table 2. Positions of A exciton and bandgap values for LPE WS_2 samples with the three different surfactants.

Surfactant	Surfactant concentration [mM]	A-exciton position [nm]	Bandgap [eV]
	8.2	629.3	1.74
	4.1	629.3	1.74
SDS	2.0	630.3	1.61
	1.0	630.9	1.67
	0.5	632.1	1.42
	8.2	629.3	1.74
	4.1	629.3	1.74
SDBS	2.0	628.2	1.75
	1.0	628.2	1.74
	0.5	630.3	1.70
	8.2	628.2	1.43
	4.1	630.3	1.70
SHS	2.0	629.3	1.75
	1.0	629.3	1.75
	0.5	629.3	1.75

Table 3. Distance between E_{2g} and A_{1g} Raman peaks in LPE MoS_2 samples.

Surfactant	Surfactant concentration [mM]	$\Delta\nu$ [cm^{-1}]
	8.2	24.4
	4.1	25.1
SDS	2.0	24.6
	1.0	25.7
	0.5	25
	8.2	25
	4.1	24.9
SDBS	2.0	25.1
	1.0	25.0
	0.5	25.4
	8.2	25
	4.1	25
SHS	2.0	25
	1.0	25
	0.5	25.5

For monolayered MoS_2, at an excitation wavelength of 532 nm, a difference between the A_{1g} and the E_{2g} peak at 18 cm^{-1} is expected. Few layered materials have shifts from 18 to 25 cm^{-1}. Above 25 cm^{-1} samples are expected to be multilayered/bulk-like material. In **Table 3**, the distance of the two Raman peaks is shown for all samples with the three different surfactants and from 0.5 up to 8.2 mM. Apart from SDS 8.2 mM, SDS 2.0 mM, and SDBS 4.1 mM, all other samples show a shift of 25 cm^{-1} or bigger, which is a characteristic of a multilayered material. However, it is important to consider that a certain degree of restacking of the layers is expected during sample preparation, since for the Raman analysis the suspensions are evaporated and the residual dried particles are measured.[47]

Figure 5d–f summarizes the Raman spectra of all the exfoliated WS_2 samples. For all the samples, the peaks relative to

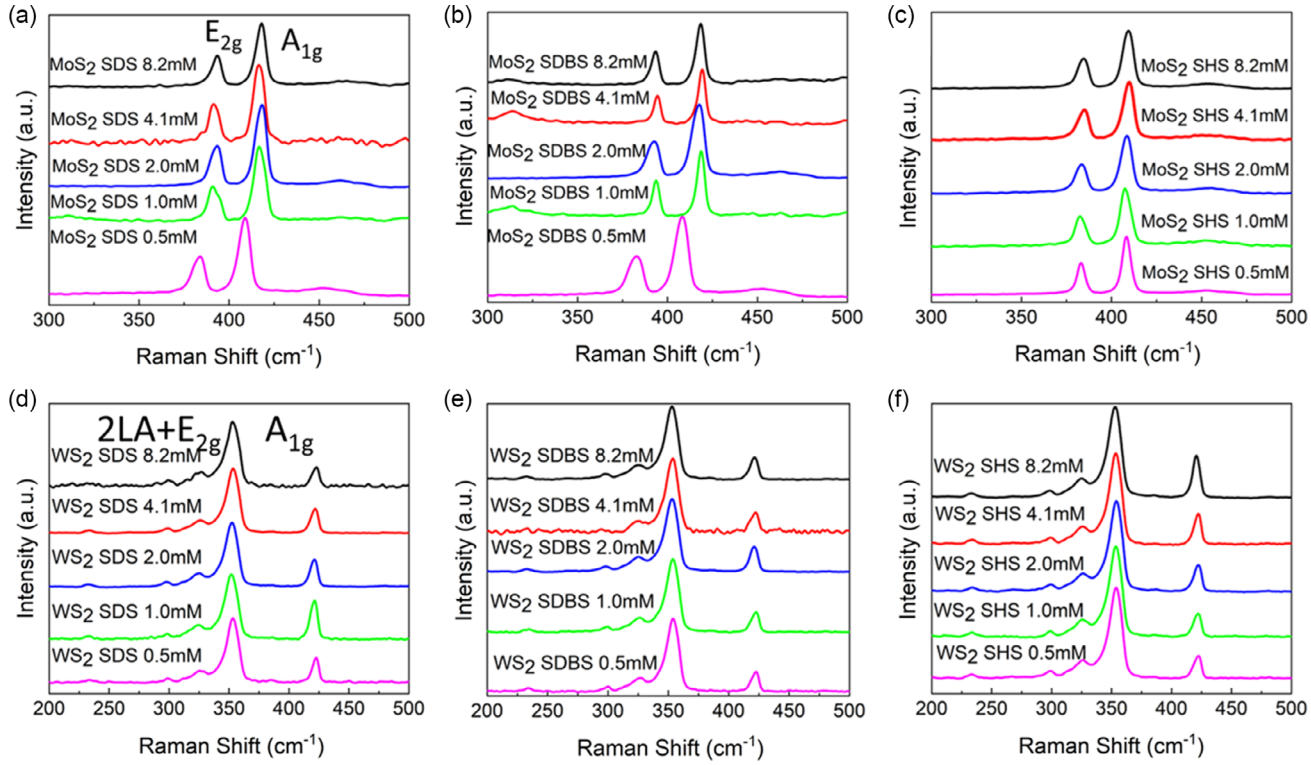

Figure 5. Raman spectra of LPE a–c) MoS_2 and d–f) WS_2.

Table 4. $(2LA + E_{2g})/A_{1g}$ ratios in LPE WS_2 samples.

Surfactant	Surfactant concentration [mM]	$(2LA + E_{2g})/A_{1g}$ ratio
	8.2	3.38
	4.1	2.66
SDS	2.0	2.35
	1.0	1.69
	0.5	2.58
	8.2	3.67
	4.1	3.67
SDBS	2.0	2.90
	1.0	3.81
	0.5	3.34
	8.2	2.17
	4.1	3.00
SHS	2.0	3.40
	1.0	3.90
	0.5	4.05

Table 5. Product concentration and yield for LPE MoS_2 calculated from Lambert–Beer law and from weighted freeze-dried samples.

Surfactant	Surfactant concentration [mM]	Product concentration by UV–vis absorption [mg mL^{-1}]	Product concentration by freeze-drying [mg mL^{-1}]	Yield [%]
	8.2	0.028		0.28
	4.1	0.051		0.51
SDS	2.0	0.077		0.77
	1.0	0.021		0.21
	0.5	0.027		0.27
	8.2	0.085		0.85
	4.1	0.08		0.8
SDBS	2.0	0.093		0.93
	1.0	0.11		1.1
	0.5	0.043		0.43
	8.2	0.032	0.36	0.32
	4.1	0.042		0.42
SHS	2.0	0.027	1.35	0.27
	1.0	0.021		0.21
	0.5	0.061		0.61

$2LA + E_{2g}$ and A_{1g} vibrational modes can be observed, at around 355 and 417 cm^{-1}, respectively.[48,49] As reported by other works present in the literature, the increasing ratio of $(2LA + E_{2g})/A_{1g}$ is due to the decreasing the atomic layers of WS_2 nanosheets.[50] For bulk WS_2, the $(2LA + E_{2g})/A_{1g}$ ratio is around 0.5, while the ratio of monolayered WS_2 reaches above 2. When the ratio value is between 1 and 2, WS_2 nanosheets are present as few-layer-stacked particle layers.[51] As shown in Figure 5d–f and **Table 4**, independent from the type and concentration of the surfactant, all the exfoliated WS_2 samples are adequate for producing monolayer WS_2, except the case of SDS at a concentration of 1.0 mM where a few-layered system was obtained. This might be due to the restacking of the exfoliated samples during the preparation and Raman spectroscopy measurement. In general, for WS_2, we were able to show that all surfactants can produce water-based WS_2 suspension containing highly exfoliated nanosheets and the effect of restacking of the nanosheets is not apparent at the solid state.

ZP measurements were performed to characterize the stability of the obtained colloidal suspensions after LPE. As shown in **Figure 6**, all the samples of MoS_2 and WS_2 provide a ZP value lower than −20 mV, indicating that all the suspensions are colloidally stable and the suspended nanosheets negatively charged. However, when the ZP values are between −20 and −30 mV, the samples show a short-term stability, and a gradual sedimentation of materials was observed after several days. While samples with −30 mV ZP values show a long-term stability up to several months.[52] Specifically, for MoS_2, the application of SDS and SDBS mostly results in a short-term stability, independently from the surfactant concentration, since the ZP values are in the range of −20 and −30 mV, while SHS can increase the stability of the suspension dramatically, with the ZP values of SHS as −30 mV. In contrast, WS_2 suspensions show long-term stability with most of the investigated surfactants and concentrations, except with 1.0 mM SDS. Interestingly, the blue lines in Figure 6 clearly show that with SHS, the suspensions of both MoS_2 and WS_2 gain better stability than that of SDS and SDBS. When studying the impact of surfactant nature on the colloidal stability of the suspensions, no strict rule can be concluded by comparing

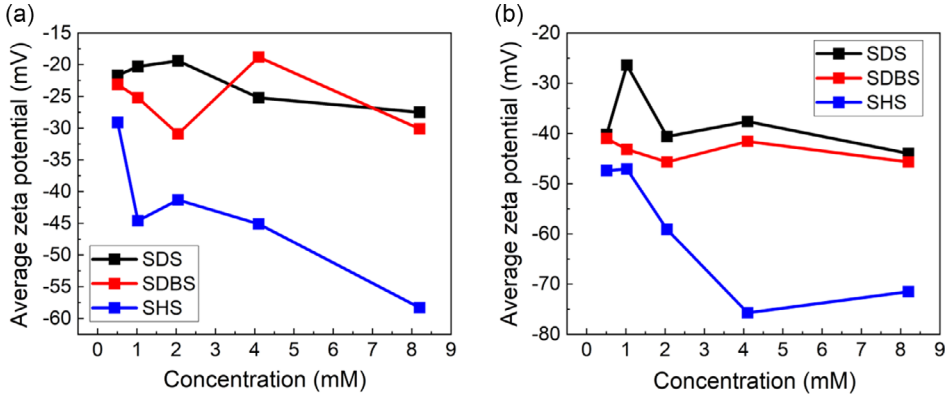

Figure 6. ZP trends for a) MoS_2 and b) WS_2 samples with different type and concentration of surfactants.

Table 6. Product concentration and yield for LPE WS_2 calculated from Lambert–Beer law and from weighted freeze-dried samples.

Surfactant	Surfactant concentration [mM]	Product concentration by UV–vis absorption [mg mL^{-1}]	Product concentration by freeze-drying [mg mL^{-1}]	Yield [%]
	8.2	0.068		0.68
	4.1	0.097		0.97
SDS	2.0	0.13	0.23	1.3
	1.0	0.11		1.1
	0.5	0.23		2.3
	8.2	0.12	1.25	0.85
	4.1	0.12		0.8
SDBS	2.0	0.14		0.93
	1.0	0.11		1.1
	0.5	0.12		1.2
	8.2	0.33	0.56	3.3
	4.1	0.11		1.1
SHS	2.0	0.12		1.2
	1.0	0.10		1.0
	0.5	0.098		0.98

the variable parameters. However, there is still a rough trend showing that, with all the surfactants used for MoS_2 and WS_2 exfoliation, higher concentrations increase the colloidal stability of the samples.

The yield in the exfoliated material is another important standard to evaluate the effect of the surfactants and the corresponding experimental parameters used. As described in Section "Calculation Methods of the Sample Concentration," UV–vis spectra are used to quantify the yield and final concentration of each suspension. The product concentration and the corresponding yield of MoS_2 and WS_2 are calculated and listed in **Table 5** and **6**, respectively. The product concentration values changed with surfactant type and concentration, as shown from the trends reported in **Figure 7**. For MoS_2 inks, SDBS results in a better product concentration, compared to the other two surfactants. With a surfactant concentration of 1.0 mM, it was possible to obtain an optimized MoS_2 concentration of 0.11 mg mL^{-1} and the highest yield of 1.1%. In contrast, for WS_2 inks there is no clear evidence showing that the type or the concentration of the surfactants has a relationship with the product concentration and yield. However, we are still able to find the best parameter with SHS 8.2 mM, which can result in an outstanding product concentration of 0.33 mg mL^{-1} and yield of 3.3% compared to other surfactant parameters. These results are comparable to the published works.[53,54] Meanwhile, for some selected samples with relatively high concentration, we were able to obtain the actual concentration from freeze-drying the suspensions. Interestingly, the concentration calculated from freeze-drying method is higher than the concentration obtained from UV–vis spectra. This might be due to the presence of residual surfactants left on the samples after prolonged dialysis, which indicates that the surfactant is tightly anchored on the nanosheet surfaces. These surfactants are necessary to hinder the aggregation of the exfoliated layers when the samples are extracted from inks, though they might influence the future application of the exfoliated products.[55]

3. Conclusion

In conclusion, a systematic study was conducted on the surfactant-assisted LPE of MoS_2 and WS_2 in water. With the aid of three different ionic surfactants (SDS, SDBS, and SHS), exfoliations were carried out in water to produce sustainable colloidal suspensions. By charactering the samples with different techniques, we were able to compare the quality of the exfoliated 2D MoS_2 and WS_2 nanosheets contained in the inks in terms of layer thickness, colloidal stability, and product yield.

For MoS_2, since most experimental parameters result in multilayer samples, the best parameters can be chosen considering the sample stability and product yield. Specifically, 8.2 mM SHS results in the best stability for LPE MoS_2 suspensions, while 1.0 mM SDBS can result in the highest yield of the product. Depending on the target application for the produced ink, one can thus decide whether to proceed with a colloid containing surfactant amount, which is relevant for certain purposes such as use in electronic or energy-related applications.

As for what concerns LPE WS_2, almost all the parameter combinations result in monolayered product, except 8.2 mM SHS, which anyway provides the highest yield in suspended WS_2. And, 4.1 mM SHS is likely the preferred choice to provide the

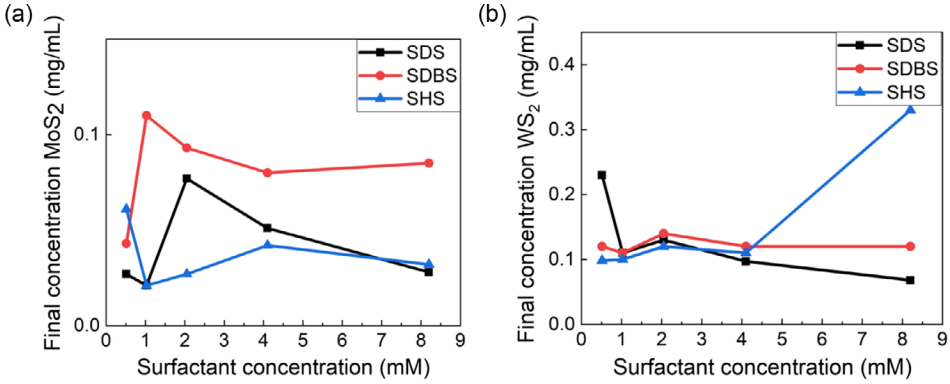

Figure 7. Product concentration trends for a) LPE MoS_2 and b) LPE WS_2 samples.

most stable suspension of layered WS_2 in water. Considering that the CMC of SHS is only 0.55 mM, our results surprisingly indicate that the best concentration of SHS in the LPE of MoS_2 and WS_2 is indeed highly above the CMC. As to the product yield, the all the experiments reported in this work obtain a yield of less than 3.3%, which is comparable but does not outperform other published works. Therefore, modifications such as new surfactants with different length of carbon chains and functional groups, or longer exfoliation time, are necessary to increase the product yield. With the detailed provision of a wide scenario of experimental conditions from which to select one's needs for a specific application, such as processing of thin films, nanochemistry, or even biomedicine, this study will constitute a useful tool for further research in the field of sustainable production of 2D material inks.

4. Experimental Section

Materials and LPE Process: MoS_2 (99%), WS_2 (99%), SDS, and SDBS were purchased from Sigma Aldrich and used without further purification. SHS was purchased from TCI Chemicals and used without further purification. All the exfoliations were performed using a tip sonicator and the samples were cooled down to 0 °C with an ice bath during the process. LPE was carried out on a Bandelin Sonopuls tip sonicator, operating with 80% power using pulses of 1 s on/1 s off for 4 h. In all the experiments, the suspension volume was kept fixed at 150 mL with a concentration of the bulk materials of 10 mg mL^{-1}. The concentration of all the surfactants was 8.2, 4.1, 2.0, 1.0, and 0.5 mM. After the sonication step, liquid cascade centrifugation was applied at two different rates. The suspensions obtained after the sonication were centrifuged for 30 min at 1500 rpm and, after keeping the supernatants, those were further centrifuged for 30 min at 3000 rpm with a Universal 320 Hettich centrifuge. Ultrapure water was obtained with the Milli-Q Direct Water Purification System. The detailed parameters of all the experiments performed in this work are listed in Table S1, Supporting Information.

Characterization: UV–visible (UV–vis) absorption spectra of the colloidal inks were recorded on a Goebel Uvikon spectrometer using a quartz cuvette of 1 cm optical length from 350 to 1000 nm with a scan interval of 0.25 nm. Raman spectra were recorded on a Bruker Senterra instrument using a 532 nm laser excitation source with a 2 mW of power, 6 s of integration, and 60 co-additions. The samples were prepared by drop-casting the suspensions over a silicon slide and then analyzed. ZP was measured on a Malvern Zetasizer Nano-ZS device three times and the results were averaged to obtain the final results. The samples were measured in Rotilabo precision glass cuvettes with a light path of 10 mm and a volume of 3.5 mL. TEM images were recorded using a non-aberration-corrected TALOS F200X (ThermoScientific, Eindhoven, Netherland) operated at 200 kV. Images were recorded on a 16Mpxls CMOS camera with a 1 s exposure time.

Calculation Methods of the Sample Concentration: UV analysis was employed to calculate the final concentration of the 2D materials. A calibration line was obtained using a set of dilutions from a suspension with a known concentration, obtained after filtration. The slope of the calibration line corresponded to the extinction coefficient of the dispersed material. The final concentrations of the MoS_2 and WS_2 were obtained with the Lambert–Beer law (Equation (2))

$$A = \varepsilon bc \tag{2}$$

where A stands for absorbance of the material, ε is the extinction coefficient of the dispersed nanosheets, and c is the concentration of the suspension. In this work, we used the absorption value of the A exciton as A. ε was obtained from the calibration lines from several standard MoS_2 and WS_2 suspensions with known concentrations. For MoS_2, the calculated ε was 7.85 mg mL^{-1} cm, while for WS_2 the ε was 3.91 mg mL^{-1} cm.

The other method used to obtain the final concentration was freeze-drying. Before freeze-drying, dialysis was performed using cellulose dialysis bag (Carl Roth) 14 kDa, filling each bag with 20–25 mL of the desired suspension and closing both sides with a plastic pin once filled. The bag was then left in a suitable Becker with Milli-Q water for 3 days, changing 3 times per day the water. Freeze-drying was performed at −10 °C for 16 h and a pressure of 1 mPa.

Supporting Information

Supporting Information is available from the Wiley Online Library or from the author.

Acknowledgements

M.P., F.B., and M.C. contributed equally to this work. This research was funded by the ERC StG project JANUS BI (grant agreement no. 101041229). M.W. and T.G. also thank Fondazione Compagnia di San Paolo for financial support through the "Bando TRAPEZIO - Paving the way to research excellence and talent attraction". T.G. further acknowledges Fondazione Compagnia di San Paolo for the support through the Starting Grant ERC program. M.C., F. B., and T.G. also acknowledge the support of the European Commission through the H2020 FET-PROACTIVE-EIC-07-2020 project LIGHT-CAP (grant no. 101017821). The authors declare no conflict of interest.

Conflict of Interest

The authors declare no conflict of interest.

Data Availability Statement

The data that support the findings of this study are available from the corresponding author upon reasonable request.

Keywords

2D materials, colloidal inks, green chemistry, surfactant-assisted liquid-phase exfoliations, sustainabilities, transition-metal dichalcogenides

Received: January 31, 2024
Revised: February 20, 2024
Published online: March 4, 2024

[1] S. Ott, N. Wolff, F. Rashvand, V. J. Rao, J. Zaumseil, C. Backes, *Chem. Mater.* **2019**, *31*, 8424.
[2] X. Geng, J. Yi, *Nano-Sized Multifunctional Materials: Synthesis, Properties and Applications*, Elsevier, Amsterdam **2019**, pp. 117–144.
[3] Y. Guan, H. Yao, H. Zhan, H. Wang, Y. Zhou, J. Kang, *RSC Adv.* **2021**, *11*, 14085.
[4] C. Nie, J. Wang, B. Cai, B. Lai, S. Wang, Z. Ao, *Appl. Catal., B* **2024**, *340*, 123173.
[5] Z. Liang, R. Shen, Y. H. Ng, P. Zhang, Q. Xiang, X. Li, *J. Mater. Sci. Technol.* **2020**, *56*, 89.
[6] A. Sebastian, R. Pendurthi, T. H. Choudhury, J. M. Redwing, S. Das, *Nat. Commun.* **2021**, *12*, 693.
[7] C. Lan, C. Li, J. C. Ho, Y. Liu, *2D WS2: From Vapor Phase Synthesis to Device Applications*, Vol. *7*, Blackwell Publishing Ltd., Hoboken **2021**.

[8] M. H. Kang, D. Lee, J. Sung, J. Kim, B. H. Kim, J. Park, *Comprehensive Nanoscience and Nanotechnology*, Elsevier, Amsterdam **2019**, pp. 55–90.
[9] S. Pinilla, J. Coelho, K. Li, J. Liu, V. Nicolosi, *Two-Dimensional Material Inks*, Vol. *7*, Nature Research, London **2022**, pp. 717–735.
[10] J. N. Coleman, M. Lotya, A. O'neill, S. D. Bergin, P. J. King, U. Khan, K. Young, A. Gaucher, S. De, R. J. Smith, I. V. Shvets, S. K. Arora, G. Stanton, H.-Y. Kim, K. Lee, G. T. Kim, G. S. Duesberg, T. Hallam, J. J. Boland, J. J. Wang, J. F. Donegan, J. C. Grunlan, G. Moriarty, A. Shmeliov, R. J. Nicholls, J. M. Perkins, E. M. Grieveson, K. Theuwissen, D. W. Mccomb, P. D. Nellist, et al., *Science* **2011**, *331*, 568.
[11] R. J. Smith, P. J. King, M. Lotya, C. Wirtz, U. Khan, S. De, A. O'Neill, G. S. Duesberg, J. C. Grunlan, G. Moriarty, J. Chen, J. Wang, A. I. Minett, V. Nicolosi, J. N. Coleman, *Adv. Mater.* **2011**, *23*, 3944.
[12] M. Chhowalla, H. S. Shin, G. Eda, L. J. Li, K. P. Loh, H. Zhang, *Nat. Chem.*, **2013**, *5*, 263.
[13] C. Backes, T. M. Higgins, A. Kelly, C. Boland, A. Harvey, D. Hanlon, J. N. Coleman, *Guidelines for Exfoliation, Characterization and Processing of Layered Materials Produced by Liquid Exfoliation*, Vol. *29*, American Chemical Society, Washington **2017**, pp. 243–255.
[14] Y. Xu, H. Cao, Y. Xue, B. Li, W. Cai, *Liquid-Phase Exfoliation of Graphene: An Overview on Exfoliation Media, Techniques, and Challenges*, Vol. *8*, MDPI AG, Basel **2018**.
[15] Z. Li, R. J. Young, C. Backes, W. Zhao, X. Zhang, A. A. Zhukov, E. Tillotson, A. P. Conlan, F. Ding, S. J. Haigh, K. S. Novoselov, J. N. Coleman, *ACS Nano* **2020**, *14*, 10976.
[16] A. Jawaid, D. Nepal, K. Park, M. Jespersen, A. Qualley, P. Mirau, L. F. Drummy, R. A. Vaia, *Chem. Mater.* **2016**, *28*, 337.
[17] C. X. Hu, Y. Shin, O. Read, C. Casiraghi, *Dispersant-Assisted Liquid-Phase Exfoliation of 2D Materials Beyond Graphene*, Vol. *13*, Royal Society of Chemistry, London **2021**, pp. 460–484.
[18] H. Tao, Y. Zhang, Y. Gao, Z. Sun, C. Yan, J. Texter, *Scalable Exfoliation and Dispersion of Two-Dimensional Materials-An Update*, Vol. *19*, Royal Society of Chemistry, London **2017**, pp. 921–960.
[19] T. Ivanković, J. Hrenović, *Arch. Ind. Hyg. Toxicol.* **2010**, *61*, 95.
[20] A. Griffin, K. Nisi, J. Pepper, A. Harvey, B. M. Szydłowska, J. N. Coleman, C. Backes, *Chem. Mater.* **2020**, *32*, 2852.
[21] Y. J. Lee, L. Huang, H. Wang, M. L. Sushko, B. Schwenzer, I. A. Aksay, J. Liu, *Colloids Interface Sci. Commun.* **2015**, *8*, 1.
[22] S. De, S. Malik, A. Ghosh, R. Saha, B. Saha, *RSC Adv.* **2015**, *5*, 65757.
[23] A. Gupta, V. Arunachalam, S. Vasudevan, *J. Phys. Chem. Lett.* **2015**, *6*, 739.
[24] H. Domínguez, *J. Phys. Chem. B* **2007**, *111*, 4054.
[25] Z. Guan, C. Wang, W. Li, S. Luo, Y. Yao, S. Yu, R. Sun, C. P. Wong, *Nanotechnology* **2018**, *29*, 425702.
[26] A. Roy, P. Kalita, B. Mondal, *J. Mater. Sci.: Mater. Electron.* **2023**, *34*.
[27] B. Zhang, M. Wang, M. Ghini, A. E. M. Melcherts, J. Zito, L. Goldoni, I. Infante, M. Guizzardi, F. Scotognella, I. Kriegel, L. De Trizio, L. Manna, *ACS Mater. Lett.* **2020**, *2*, 1442.
[28] B. Abreu, B. Almeida, P. Ferreira, R. M. F. Fernandes, D. M. Fernandes, E. F. Marques, *J. Colloid Interface Sci.* **2022**, *626*, 167.
[29] S. A. Markarian, L. R. Harutyunyan, R. S. Harutyunyan, *J. Solution Chem.* **2005**, *34*, 361.
[30] Y. Moroi, K. Motomura, R. Matuura, *The Critical Micelle Concentration of Sodium Dodecyl Sulfate-Bivalent Metal Dodecyi Sulfate Mixtures in Aqueous Solutions*.
[31] K. Yang, L. Zhu, B. Xing, *Environ. Sci. Technol.* **2006**, *40*, 4274.
[32] N. Baccile, A. Poirier, *Microbial Biobased Amphiphiles (Biosurfactants): General Aspects on CMC, Surface Tension and Phase Behaviour*, Vol. *1*, Elsevier, Amsterdam **2022**, pp. 1–38.
[33] G. Solomon, R. Mazzaro, V. Morandi, I. Concina, A. Vomiero, *Crystals* **2020**, *10*, 1.
[34] H. C. Kim, H. Kim, J. U. Lee, H. B. Lee, D. H. Choi, J. H. Lee, W. H. Lee, S. H. Jhang, B. H. Park, H. Cheong, S. W. Lee, H. J. Chung, *ACS Nano* **2015**, *9*, 6854.
[35] A. Eghbali, A. A. Vyshnevyy, A. V. Arsenin, V. S. Volkov, *Biosensors* **2022**, *12*, 582.
[36] C. Backes, K. R. Paton, D. Hanlon, S. Yuan, M. I. Katsnelson, J. Houston, R. J. Smith, D. McCloskey, J. F. Donegan, J. N. Coleman, *Nanoscale* **2016**, *8*, 4311.
[37] A. Griffin, A. Harvey, B. Cunningham, D. Scullion, T. Tian, C. J. Shih, M. Gruening, J. F. Donegan, E. J. G. Santos, C. Backes, J. N. Coleman, *Chem. Mater.* **2018**, *30*, 1998.
[38] T. P. Nguyen, W. Sohn, J. H. Oh, H. W. Jang, S. Y. Kim, *J. Phys. Chem. C* **2016**, *120*, 10078.
[39] S. M. Winata, V. Fauzia, in *Journal of Physics: Conf. Series*, Institute of Physics, Bristol **2022**.
[40] G. A. Ermolaev, Y. V. Stebunov, A. A. Vyshnevyy, D. E. Tatarkin, D. I. Yakubovsky, S. M. Novikov, D. G. Baranov, T. Shegai, A. Y. Nikitin, A. V. Arsenin, V. S. Volkov, *NPJ 2D Mater. Appl.* **2020**, *4*, 21.
[41] G. S. Bang, K. W. Nam, J. Y. Kim, J. Shin, J. W. Choi, S. Y. Choi, *ACS Appl. Mater. Interfaces* **2014**, *6*, 7084.
[42] T. Krasian, W. Punyodom, P. Worajittiphon, *Chem. Eng. J.* **2019**, *369*, 563.
[43] H. Li, Q. Zhang, C. C. R. Yap, B. K. Tay, T. H. T. Edwin, A. Olivier, D. Baillargeat, *Adv. Funct. Mater.* **2012**, *22*, 1385.
[44] B. Adilbekova, Y. Lin, E. Yengel, H. Faber, G. Harrison, Y. Firdaus, A. El-Labban, D. H. Anjum, V. Tung, T. D. Anthopoulos, *J. Mater. Chem* **2020**, *8*, 5259.
[45] B. Chakraborty, H. S. S. R. Matte, A. K. Sood, C. N. R. Rao, *J. Raman Spectrosc.* **2013**, *44*, 92.
[46] M. W. Iqbal, K. Shahzad, R. Akbar, G. Hussain, *Microelectron. Eng.* **2020**, *219*, 111152.
[47] Y. Zhao, Y. Sun, M. Bai, S. Xu, H. Wu, J. Han, H. Yin, C. Guo, Q. Chen, Y. Chai, Y. Guo, *J. Phys. Chem. C* **2020**, *124*, 11092.
[48] H. R. Gutiérrez, N. Perea-López, A. L. Elías, A. Berkdemir, B. Wang, R. Lv, F. López-Urías, V. H. Crespi, H. Terrones, M. Terrones, *Nano Lett.* **2013**, *13*, 3447.
[49] A. Berkdemir, H. R. Gutiérrez, A. R. Botello-Méndez, N. Perea-López, A. L. Elías, C. I. Chia, B. Wang, V. H. Crespi, F. López-Urías, J. C. Charlier, H. Terrones, M. Terrones, *Sci. Rep.* **2013**, *3*, 1755.
[50] M. Crisci, F. Boll, L. Merola, J. J. Pflug, Z. Liu, J. Gallego, F. Lamberti, T. Gatti, *Front. Chem.* **2022**, *10*, 1.
[51] A. M. Abdelkader, I. A. Kinloch, *ACS Sustainable Chem. Eng.* **2016**, *4*, 4465.
[52] J. Kim, S. Kwon, D. H. Cho, B. Kang, H. Kwon, Y. Kim, S. O. Park, G. Y. Jung, E. Shin, W. G. Kim, H. Lee, G. H. Ryu, M. Choi, T. H. Kim, J. Oh, S. Park, S. K. Kwak, S. W. Yoon, D. Byun, Z. Lee, C. Lee, *Nat. Commun.* **2015**, *6*, 8294.
[53] D. Sahoo, B. Kumar, J. Sinha, S. Ghosh, S. S. Roy, B. Kaviraj, *Sci. Rep.* **2020**, *10*, 10759.
[54] L. Ma, Z. Liu, Z. L. Cheng, *Ceram. Int.* **2020**, *46*, 3786.
[55] C. Verma, C. M. Hussain, M. A. Quraishi, A. Alfantazi, *Green Surfactants For Corrosion Control: Design, Performance and Applications*, Vol. *311*, Elsevier B.V., Amsterdam **2023**.